

Inhibition by *Jasminum nudiflorum* Lindl. leaves extract of the corrosion of cold rolled steel in hydrochloric acid solution

Xiang-Hong Li · Shu-Duan Deng · Hui Fu

Received: 20 November 2009 / Accepted: 18 May 2010 / Published online: 4 June 2010
© Springer Science+Business Media B.V. 2010

Abstract The inhibition effect of *Jasminum nudiflorum* Lindl. leaves extract (JNLLE) on the corrosion of cold rolled steel (CRS) in 1.0 M hydrochloric acid (HCl) was investigated by weight loss, potentiodynamic polarization, and electrochemical impedance spectroscopy (EIS) methods. The results show that JNLLE acts as a very good inhibitor, and the inhibition efficiency increases with the concentration of JNLLE. The adsorption of JNLLE obeys Langmuir adsorption isotherm. Values of inhibition efficiency obtained from weight loss, potentiodynamic polarization, and electrochemical impedance spectroscopy (EIS) are in good agreement. Polarization curves show that JNLLE behaves as a mixed-type inhibitor in hydrochloric acid. EIS shows that charge-transfer resistance increase and the capacitance of double layer decreases with the inhibitor concentration, confirming the adsorption process mechanism. The adsorbed film on CRS surface containing JNLLE inhibitor was also measured by Fourier transform infrared spectroscopy (FTIR) and scanning electron microscope (SEM). A probable inhibitive mechanism is proposed from the viewpoint of adsorption theory.

Keywords *Jasminum nudiflorum* Lindl. · Corrosion inhibitor · Hydrochloric acid · Cold rolled steel · Polarization · EIS · FTIR · SEM

X.-H. Li (✉) · H. Fu
Department of Fundamental Courses, Southwest Forestry University, Kunming 650224, People's Republic of China
e-mail: xianghong-li@163.com

S.-D. Deng
Faculty of Wood Science and Decoration Engineering, Southwest Forestry University, Kunming 650224, People's Republic of China

1 Introduction

The corrosion of steel is a fundamental academic and industrial concern, which has received a considerable amount of attention [1]. The use of inhibitors is one of the most practical methods for protection against corrosion, especially in acidic media [2]. Acid solutions are widely used in industry, some of the important fields of application being acid pickling, chemical cleaning and processing, ore production, and oil well acidification. As acidic media, the use of hydrochloric acid (HCl) in pickling of metals, acidization of oil wells and in cleaning of scales is more economical, efficient, and trouble-free, compared to other mineral acids [3]. Because of the general aggression of acid solutions, inhibitors are used to prevent metal dissolution as well as acid consumption. The book including extensive listing of various types of organic inhibitors has been published [4]. Among numerous inhibitors that have been tested and applied industrially as corrosion inhibitors, those that are non-toxic or low-toxic are now far more strategic than in the recent past. In the twenty-first century, the research in the field of “green” or “eco-friendly” corrosion inhibitors has been addressed toward the goal of using cheap, effective compounds at low or “zero” environmental impact.

Plant extract is low in cost and environmentally safe, and so the main advantage in the use of plant extract as corrosion inhibitor is due to both economic and environmental benefits. Up to now, many plant leaves extract have been used as effective corrosion inhibitors of iron or steel in acidic media, such as *Azadirachta* [5], *Vernonia amygdalina* [6], henna [7, 8], *Nypha fruticans* Wurmb [9], *Zanthoxylum alatum* [10, 11], Damsissa [12], *Mentha pulegium* [13], olive [14], *Phyllanthus amarus* [15], *Occimum viridis* [16, 17], lupine [18], *Lasianthera africana*

[19], and *Strychnos nux-vomica* [20]. The inhibition performance of plant extract is normally ascribed to the presence in their composition of complex organic species such as tannins, alkaloids and nitrogen bases, carbohydrates, and proteins as well as hydrolysis products [16]. These organic compounds contain polar functions with nitrogen, sulfur, or oxygen atoms as well as those with triple or conjugated double bonds or aromatic rings in their molecular structures, which are the major adsorption centers. However, literature reveals that study on the use of extract of *Jasminum nudiflorum* Lindl. leaves as an inhibitor for the corrosion of steel is scant.

Jasminum nudiflorum Lindl. (Chinese name Yingchun-hua), a kind of defoliation shrub, belongs to family Oleaceae and genus Jasminum. In China, its original planted areas were in middle and north provinces, and it is planted in every place now [21]. *Jasminum nudiflorum* Lindl. leaves extract (JNLLE) is non-poisonous, and rich in flavonoids, secoiridoids, and fatty acid [22], and always used for dispelling heat, sweating, diuresising, activating blood, detumescence, obtunding, etc [23]. The objective of this study is to investigate the inhibition effect of JNLLE on the corrosion of cold rolled steel (CRS) in 1.0 M HCl solution for the first time by weight loss, potentiodynamic polarization, and electrochemical impedance spectroscopy (EIS) methods. Meanwhile, the steel surface was examined by Fourier transform infrared (FTIR) spectroscopy and scanning electron microscope (SEM). It is expected to get useful information on the adsorption and inhibition effects of JNLLE on steel in HCl solution.

2 Experimental method

2.1 Materials

Tests were performed on a CRS of the following composition (wt%): 0.07% C, 0.3% Mn, 0.022% P, 0.010% S, 0.01% Si, 0.030% Al, and bal. Fe.

2.2 Extraction of *Jasminum nudiflorum* Lindl. leaves

Fresh *Jasminum nudiflorum* Lindl. leaves were picked in campus of Southwest Forestry University followed by cleaning with water to eliminate ash of mud and then dried for 2 days in an oven at 60 °C and ground to powder.

The powder sample weighing 15 g was refluxed in 450 mL 80% (percent by volume) C_2H_5OH at 75 °C for 2 h. The refluxed solution was filtered, and the filtered liquor was evaporated to 100 mL of dark brown residue, and then degreased with petroleum ether and extracted with separating funnel. Thereafter, the solution was evaporated to about 50 mL dark brown residues, and dried in vacuum

drying oven at 60 °C for 2 days. Then, the dark brown solid residue was obtained after drying completely, and preserved in a desiccator. A stock solution (1,000 mg L⁻¹) with brown-red color was used to prepare the desired concentrations by dilution with distilled water.

2.3 Solutions

The aggressive solutions of 1.0 M HCl were prepared by dilution of analytical grade 37% HCl with distilled water. The concentration range of JNLLE used was 2–50 mg L⁻¹.

2.4 Weight loss measurements

The CRS sheets of 2.5 cm × 2.0 cm × 0.06 cm were abraded by a series of emery papers (grade 320-500-800) and then washed with distilled water and acetone. After weighing accurately, three parallel specimens were completely immersed in an open beaker containing 250 mL 1.0 M HCl without and with different concentrations of JNLLE at 20 °C. After 48 h, the specimens were taken out, washed, dried, and weighed accurately. The average weight loss of three parallel CRS sheets is obtained. The inhibition efficiency (E_w) is calculated as follows [24]:

$$E_w\% = \frac{W_0 - W}{W_0} \times 100 \quad (1)$$

where W_0 and W are the values of average weight loss without and with inhibitor, respectively.

2.5 Electrochemical measurements

Electrochemical experiments were carried out in a conventional three-electrode cell with a platinum counter electrode (CE) and a saturated calomel electrode (SCE) coupled to a fine Luggin capillary as the reference electrode. In order to minimize the ohmic contribution, the Luggin capillary was kept close to working electrode (WE) which was in the form of a square CRS embedded in PVC holder using epoxy resin so that the flat surface was the only surface in the electrode. The working surface area is 1.0 cm × 1.0 cm, abraded with emery paper (grade 320-500-800) on test face, rinsed with distilled water, degreased with acetone, and dried with a cold air stream. Before measurement the electrode was immersed in test solution at open circuit potential (OCP) for 2 h until a steady state was reached. All electrochemical measurements were carried out using PARSTAT 2273 advanced electrochemical system (Princeton Applied Research). Each experiment was repeated at least three times to check the reproducibility.

The potential of potentiodynamic polarization curves was increased at 30 mV min⁻¹ and started from a potential

of -250 to $+250$ mV versus free corrosion potential (E_{corr} vs. SCE). Inhibition efficiency ($E_p\%$) is defined as:

$$E_p\% = \frac{I_{\text{corr}} - I_{\text{corr}(\text{inh})}}{I_{\text{corr}}} \times 100 \quad (2)$$

where I_{corr} and $I_{\text{corr}(\text{inh})}$ represent corrosion current density values without and with inhibitor, respectively.

Electrochemical impedance spectroscopy (EIS) was carried out at OCP in the frequency range of 0.1 Hz– 100 kHz using a 10 mV peak-to-peak voltage excitation. Inhibition efficiency ($E_R\%$) is calculated using the formula:

$$E_R\% = \frac{R_{t(\text{inh})} - R_{t(0)}}{R_{t(0)}} \times 100 \quad (3)$$

where $R_{t(0)}$ and $R_{t(\text{inh})}$ are charge transfer resistance values in the absence and presence of inhibitor, respectively.

2.6 Fourier transform infrared (FTIR) spectroscopy

FTIR spectra were recorded in an AVATAR-FTIR-360 spectrophotometer (Thermo Nicolet Company, USA), which extended from $4,000$ to 400 cm $^{-1}$, using the KBr disk technique. The JNLLE was mixed with KBr and made into the disk. The CRS specimen of size 2.5 cm \times 2.0 cm \times 0.06 cm was prepared as described above (Sect. 2.4). After immersion in 1.0 M HCl with addition of 50 mg L $^{-1}$ JNLLE at 20 °C for 48 h, the specimen was cleaned with distilled water, dried with a cold air blaster. Then, the thin adsorption layer formed on steel surface was rubbed with a small amount of KBr powder in an agate mortar in a dry box, and a KBr disk was prepared using this powder.

2.7 Scanning electron microscope (SEM)

Samples of dimension 2.5 cm \times 2.0 cm \times 0.06 cm were prepared as described above (Sect. 2.4). After immersion in 1.0 M HCl without and with addition of 50 mg L $^{-1}$ JNLLE at 20 °C for 48 h, the specimens were cleaned with distilled water, dried with a cold air blaster, and then used for a Japan instrument model (Hitachi High-Tech Science Systems Corporation) S-3000N scanning electron microscope (SEM) examinations.

3 Experimental results and discussion

3.1 Weight loss measurements

Values of inhibition efficiency ($E_w\%$) obtained from weight loss for different JNLLE concentrations in 1.0 M HCl 20 °C is presented in Fig. 1. When the concentration of JNLLE is less than 10 mg L $^{-1}$, E_w increases sharply with increase in concentration, and a further increase causes no

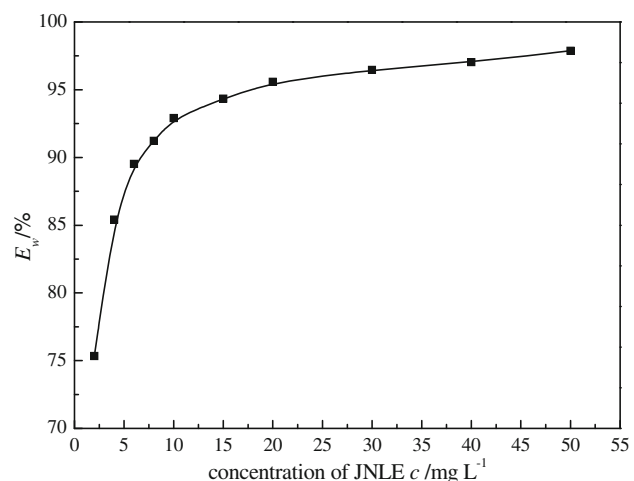


Fig. 1 Relationship between inhibition efficiency obtained from weight loss experiments (E_w) and concentration of JNLLE (c) in 1.0 M HCl

appreciable change in performance. The maximum E_w is as high as 97.9% at 50 mg L $^{-1}$, and the inhibition is estimated to be 75.3% even at very low concentration (2 mg L $^{-1}$), and at 10 mg L $^{-1}$ its protection is higher than 93% , which indicates that JNLLE acts as a very good inhibitor for CRS in 1.0 M HCl.

Assuming the inhibition action of JNLLE is caused by the adsorption of inhibitor on the CRS surface and obeys Langmuir adsorption isothermal equation [24, 25]:

$$\frac{c}{\theta} = \frac{1}{K} + c \quad (4)$$

where c is the concentration of inhibitor, K the adsorptive equilibrium constant, and θ is the surface coverage and calculated by Sekine and Hirakawa's method [26]:

$$\theta = \frac{W_0 - W}{W_0 - W_m} \quad (5)$$

where W_m is the smallest average weight loss.

Figure 2 shows the straight line of $c/\theta - c$. The linear correlation coefficient (r) is almost equal to 1 ($r = 0.9999$) and the slope is very close to 1 (slope = 0.9898), indicating the adsorption of JNLLE on steel surface follows the Langmuir adsorption isotherm. The adsorptive equilibrium constant (K) value is 1.5219 L mg $^{-1}$, which is higher than that of tween-85 (a good acid inhibitor with $K = 0.9608$ L mg $^{-1}$ at 20 °C) in the same conditions according to our recent study [27]. Thus, JNLLE is more strongly adsorbed on the steel surface in this system.

3.2 Polarization studies

Potentiodynamic polarization curves for CRS in 1.0 M HCl with various concentrations of JNLLE at 20 °C are shown

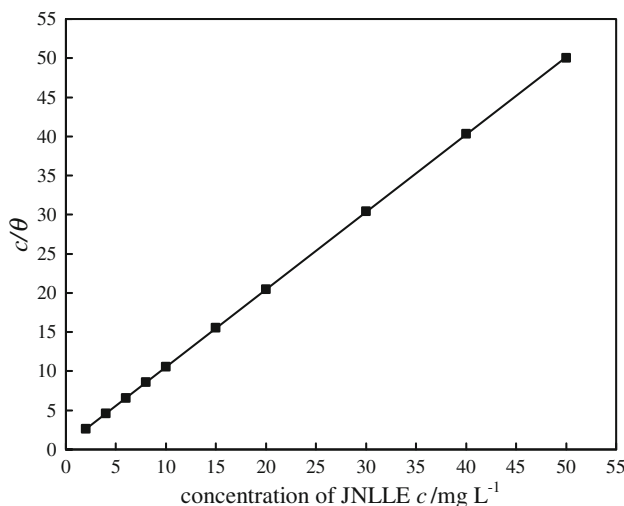


Fig. 2 The relationship between c/θ and c in 1.0 M HCl at 20 °C

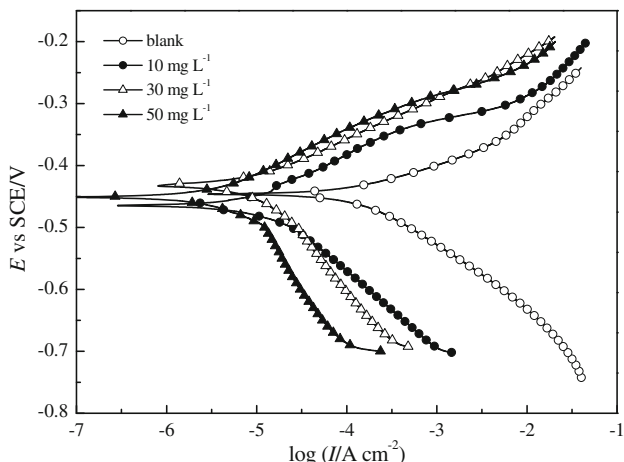


Fig. 3 Polarization curves for CRS in 1.0 M HCl containing different concentrations of JNLLE at 20 °C

in Fig. 3. The presence of inhibitor causes a remarkable decrease in the corrosion rate i.e., shifts the anodic curves to more positive potentials and the cathodic curves to more negative potentials, and to lower values of current densities. In other words, both cathodic and anodic reactions of CRS electrode corrosion are drastically inhibited by JNLLE in 1.0 M HCl. Parameters including corrosion current densities (I_{corr}), corrosion potential (E_{corr}), cathodic Tafel slope (b_c), anodic Tafel slope (b_a), and the inhibition efficiency (E_p) are listed in Table 1. Clearly, I_{corr} decreases prominently and E_p increases with the inhibitor concentration, and the maximum E_p is up to 93.0%. The presence of JNLLE does not prominently shift the E_{corr} , therefore, it can be arranged as a mixed-type inhibitor in 1.0 M HCl, and the inhibition category belongs to geometric blocking [28]. In other words, the inhibition effect comes from the reduction of the reaction area on the surface of the

corroding metal [28]. Tafel slopes of b_c and b_a change upon addition of JNLLE, which means that the inhibitor molecules are adsorbed on both anodic and cathodic sites.

3.3 Electrochemical impedance spectroscopy (EIS)

Figure 4 shows the Nyquist diagrams of CRS in 1.0 M HCl at 20 °C containing various concentrations of JNLLE after 2-h immersion. All the impedance spectra exhibit one single depressed semicircle, and the diameter of semicircle increases with the increase of inhibitor concentration. The semicircular appearance shows that the corrosion of steel is controlled by the charge transfer and the presence of inhibitor does not change the mechanism of steel dissolution [29]. Also, these impedance diagrams are not perfect semicircles which are related to the frequency dispersion as a result of the roughness and inhomogeneous of electrode surface [30]. Furthermore, it is apparent, from these plots that, the impedance response of CRS in uninhibited HCl solution has significantly changed after addition of JNLLE in the corrosive solution; as a result, real axis intercept at high and low frequencies in the presence of inhibitor is bigger than that in the absence of inhibitor (blank solution) and increases as the inhibitor concentration increases. This indicates that the impedance of inhibited substrate increases with increase in concentration of inhibitor in 1.0 M HCl.

The EIS results are simulated by the equivalent circuit shown in Fig. 5 to pure electric models that could verify or rule out mechanistic models and enable the calculation of numerical values corresponding to the physical and/or chemical properties of the electrochemical system under investigation [31]. The circuit employed allows the identification of both solution resistance (R_s) and charge transfer resistance (R_t). It is worth mentioning that the double layer capacitance (C_{dl}) value is affected by imperfections of the surface, and that this effect is simulated via a constant phase element (CPE) [32]. The CPE is composed of a component Q_{dl} and a coefficient a which quantifies different physical phenomena like surface inhomogeneity resulting from surface roughness, inhibitor adsorption, porous layer formation, etc. Therefore, the capacitance is deduced from the following relation [33]:

$$C_{dl} = Q_{dl} \times (2\pi f_{max})^{a-1} \quad (6)$$

where f_{max} represents the frequency at which imaginary value reaches a maximum on the Nyquist plot. The electrochemical parameters of R_t , CPE, a , C_{dl} and E_R are presented in Table 2.

Inspection of Table 2 reveals that R_t values increase prominently while C_{dl} reduces with the concentration of JNLLE. The decrease in C_{dl} in comparison with that in blank solution (without inhibitor), which can result from a

Table 1 Potentiodynamic polarization parameters for the corrosion of CRS in 1.0 M HCl containing different concentrations of JNLLE at 20 °C

c (mg L ⁻¹)	E_{corr} vs. SCE (mV)	I_{corr} ($\mu\text{A cm}^{-2}$)	b_c (mV dec ⁻¹)	b_a (mV dec ⁻¹)	E_p (%)
0	-446.4	134.5	101	54	—
10	-449.3	16.0	120	83	88.1
30	-431.7	12.3	182	76	90.8
50	-436.1	9.4	236	76	93.0

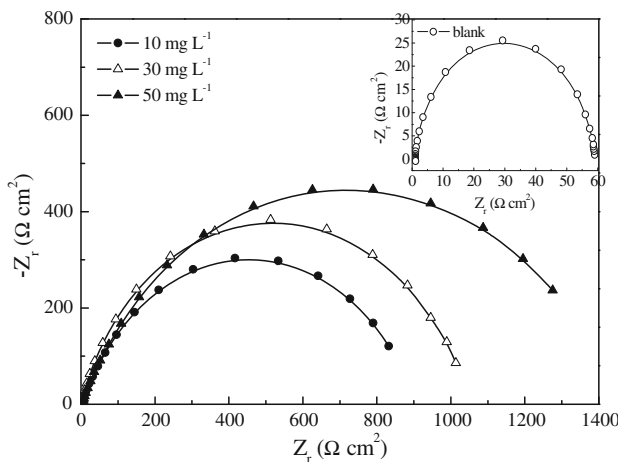


Fig. 4 EIS of the corrosion of CRS in 1.0 M HCl with different concentrations of JNLLE at 20 °C

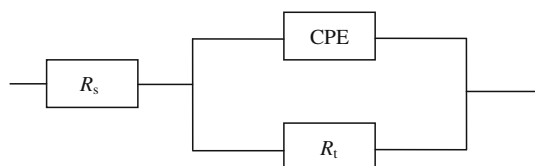


Fig. 5 The equivalent circuit model of EIS

decrease in local dielectric constant and/or an increase in the thickness of the electrical double layer, suggests that the inhibitor molecules function by adsorption at the metal/solution interface [34]. E_R increases with the concentration of JNLLE, and E_R reaches up to a maximum of 96.3%, which further confirms that JNLLE exhibits very good anti-corrosion performance.

Inhibition efficiencies obtained from weight loss (E_w), potentiodynamic polarization curves (E_p), and EIS (E_R) are in good agreement.

Table 2 EIS parameters for the corrosion of CRS in 1.0 M HCl containing JNLLE at 20 °C

c (mg L ⁻¹)	R_t (Ωcm^2)	CPE ($\mu\Omega^{-1} \text{s}^a \text{cm}^{-2}$)	a	C_{dl} ($\mu\text{F cm}^{-2}$)	E_R (%)
0	58.91	407.4	0.928	345.14	—
10	970.2	271.6	0.830	151.45	93.9
30	1090.0	225.1	0.764	83.76	94.6
50	1594.0	127.7	0.706	48.95	96.3

3.4 Corrosion inhibition kinetics

Effect of immersion time (2–144 h) on corrosion inhibition of JNLLE at 50 mg L⁻¹ in 1.0 M HCl at 20 °C was studied by weight loss and EIS methods. Table 3 shows that both corrosion rate v (weight loss method) and charge transfer resistance R_t (EIS method) act as a function of immersion time. In the absence of inhibitor, the corrosion rate is 8.42 g m⁻² h⁻¹ when the immersion time is only 2 h, then decreases slightly with the immersion time, while R_t increases with the immersion time. This result may be ascribed to the corrosion product (FeCl₂) adsorption, and the adsorption layer becomes thicker with the immersion time, which keeps steel from HCl corrosion. In the presence of 50 mg L⁻¹ JNLLE, v decreases with immersion time from 2 to 6 h, then remains constant up to 48 h, and then increases with immersion time from 48 to 144 h. The changed rule of R_t is just opposite to that of v . The results could be attributed to the formation of a protective film is time dependent on the CRS surface.

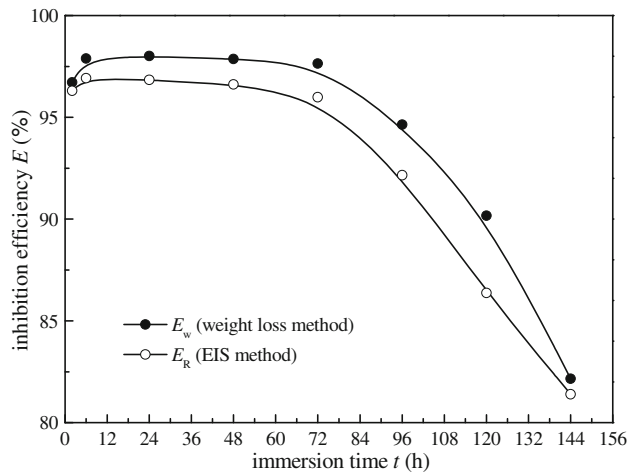
Figure 6 shows the effect of changing immersion time (2–144 h) at 20 °C on the inhibition efficiency (E) of 50 mg L⁻¹ JNLLE. Clearly, the changed rule of E obtained by weight loss and EIS methods is fairly consistent. That is, E remains constant in 2–72 h, then decreases with immersion time, and E is about 82% when the immersion time is 144 h. The decrease of E at long immersion time may be due to a deterioration of the protective layer formed in the presence of the JNLLE on the steel surface.

3.5 Fourier transform infrared spectroscopy

Several researchers [33, 35, 36] have confirmed that FTIR spectrometer is a powerful instrument that can be used to determine the type of bonding for organic inhibitors absorbed on the metal surface. In this article, FTIR spectrometer is used to identify whether there is adsorption and

Table 3 Effect of immersion time on the corrosion rate (v) and charge transfer resistance (R_t) of CRS in 1.0 M HCl at 20 °C

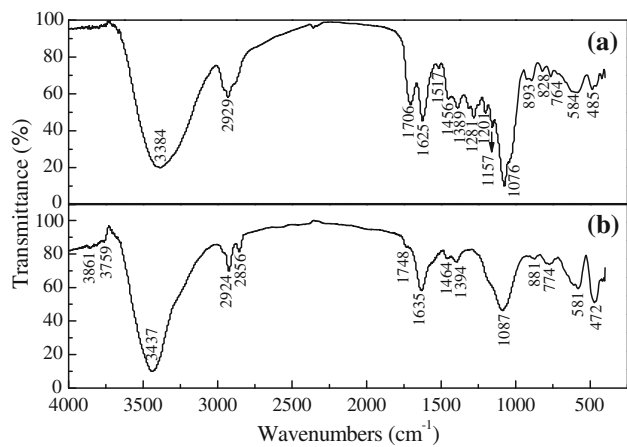
Immersion time t (h)	Corrosion rate v (g m $^{-2}$ h $^{-1}$)		Charge transfer resistance R_t (Ω cm 2)	
	Blank	50 mg L $^{-1}$ JNLLE	Blank	50 mg L $^{-1}$ JNLLE
2	8.42	0.28	58.91	1594.0
6	8.39	0.18	65.08	2113.6
24	8.10	0.16	70.34	2207.5
48	7.68	0.16	76.09	2251.8
72	7.44	0.18	81.57	2036.2
96	7.32	0.39	85.63	1091.7
120	7.25	0.71	89.64	658.4
144	7.24	1.29	92.39	490.0

**Fig. 6** Effect of immersion time (t) on the inhibition efficiency (E) obtained from both weight loss and EIS experiments with 50 mg L $^{-1}$ JNLLE in 1.0 M HCl at 20 °C

to provide new bonding information on the steel surface after immersion in inhibited HCl solution.

FTIR spectroscopy of JNLLE is shown in Fig. 7a. The strong broad band at 3,384 cm $^{-1}$ is attributed to N–H or O–H stretching. The band at 2,929 cm $^{-1}$ is related to C–H stretching vibration, and that at 1,706 cm $^{-1}$ to C=O. The strong band at 1,625 cm $^{-1}$ is assigned to C=C and C=N stretching vibration. The bands at 1,456 and 1,389 cm $^{-1}$ are attributed to C–H bending in –CH₂ and –CH₃, respectively. The absorption bands at 1517, 1281, and 1201 cm $^{-1}$ are due to the framework vibration of aromatic ring. Besides these, there are absorption bands at 1,157 and 1,076 cm $^{-1}$, which can be assigned to the C–N or C–O stretching vibration. The absorption bands below 1,000 cm $^{-1}$ are assigned to the C–H bending vibrations.

The FTIR spectrum of adsorbed protective layer formed CRS surface after 48 h immersion in 1.0 M HCl containing 50 mg L $^{-1}$ JNLLE is shown in Fig. 7b. The weak bands at 3,861 and 3,759 cm $^{-1}$ which do not appear in Fig. 7a are

**Fig. 7** FTIR spectra of **a** JNLLE **b** adsorption layer formed on the CRS surface after immersion in 1.0 M HCl + 50 mg L $^{-1}$ JNLLE for 48 h at 20 °C

assigned to Fe–O bending [33], which reveal the fact that JNLLE can adsorb on the metal surface on the basis of donor–acceptor interactions between lone-pair electrons of oxygen and the vacant d-orbital of Fe substrate. The band at 3,437 cm $^{-1}$ is attributed to O–H stretching. The weak bands at 2,924 and 2,856 cm $^{-1}$ are attributed to the aliphatic C–H asymmetric and symmetric stretching vibrations, respectively. The C=O weak stretching vibration at 1,748 cm $^{-1}$ and the C=C (or C=N) stretching vibration at 1,635 cm $^{-1}$ shifting to higher wavenumber may be due to formation of the complex of Fe $^{2+}$ –JNLLE and adsorb on steel surface. The band at 1,464 cm $^{-1}$ is attributed to –CH₂, and that at 1,394 cm $^{-1}$ to –CH₃. In addition, it should be noted that the strong band at 1,087 cm $^{-1}$ is the stretching vibration in C–N or C–O. The bands at 881 and 472 cm $^{-1}$ are due to Fe–N–H and Fe–N stretching vibration, respectively [37]. The results could suggest the presence of a trace of the JNLLE complex with Fe $^{2+}$ on the surface. Comparing Fig. 7a and b, it can be suggested that JNLLE is absorbed on the CRS surface.

3.6 Scanning electron microscope (SEM)

The SEM images of CRS surface in 1.0 M HCl are shown in Fig. 8. It can be seen from Fig. 8a that the CRS steel samples before immersion seem smooth and show some abrading scratches on the surface. However, a “black-

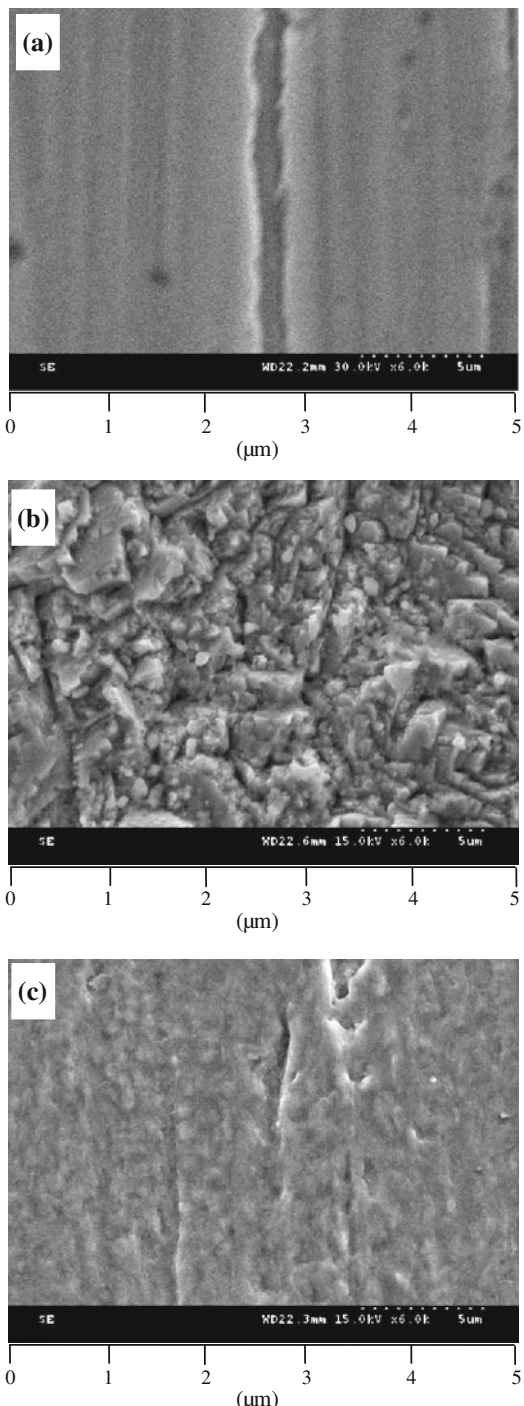
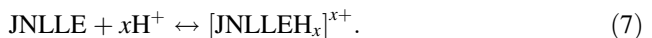


Fig. 8 SEM micrographs of CRS surface: **a** before immersion; **b** after 48 h of immersion at 20 °C in 1.0 M HCl; **c** after 48 h of immersion at 20 °C in 50 mg L⁻¹ JNLLE + 1.0 M HCl

value-like” huge appears in the middle of the surface, which is probably an oxide inclusion. There are also small black holes on steel surface, which may be attributed to the defect of steel. Inspection of Fig. 8b reveals that the CRS surface after immersion in uninhibited 1.0 M HCl for 48 h shows an aggressive attack of the corroding medium on the steel surface. The corrosion products appear very uneven and lepidoteral-like morphology, and the surface layer is rather rough. In contrast, in the presence of 50 mg L⁻¹ JNLLE, Fig. 8c shows that there is an adsorbed film adsorbed on specimen’s surface exposed to 1.0 M HCl solutions containing JNLLE, which do not exist in the Fig. 8b. In accordance, it might be concluded that the adsorption film can efficiently inhibit the corrosion of steel.

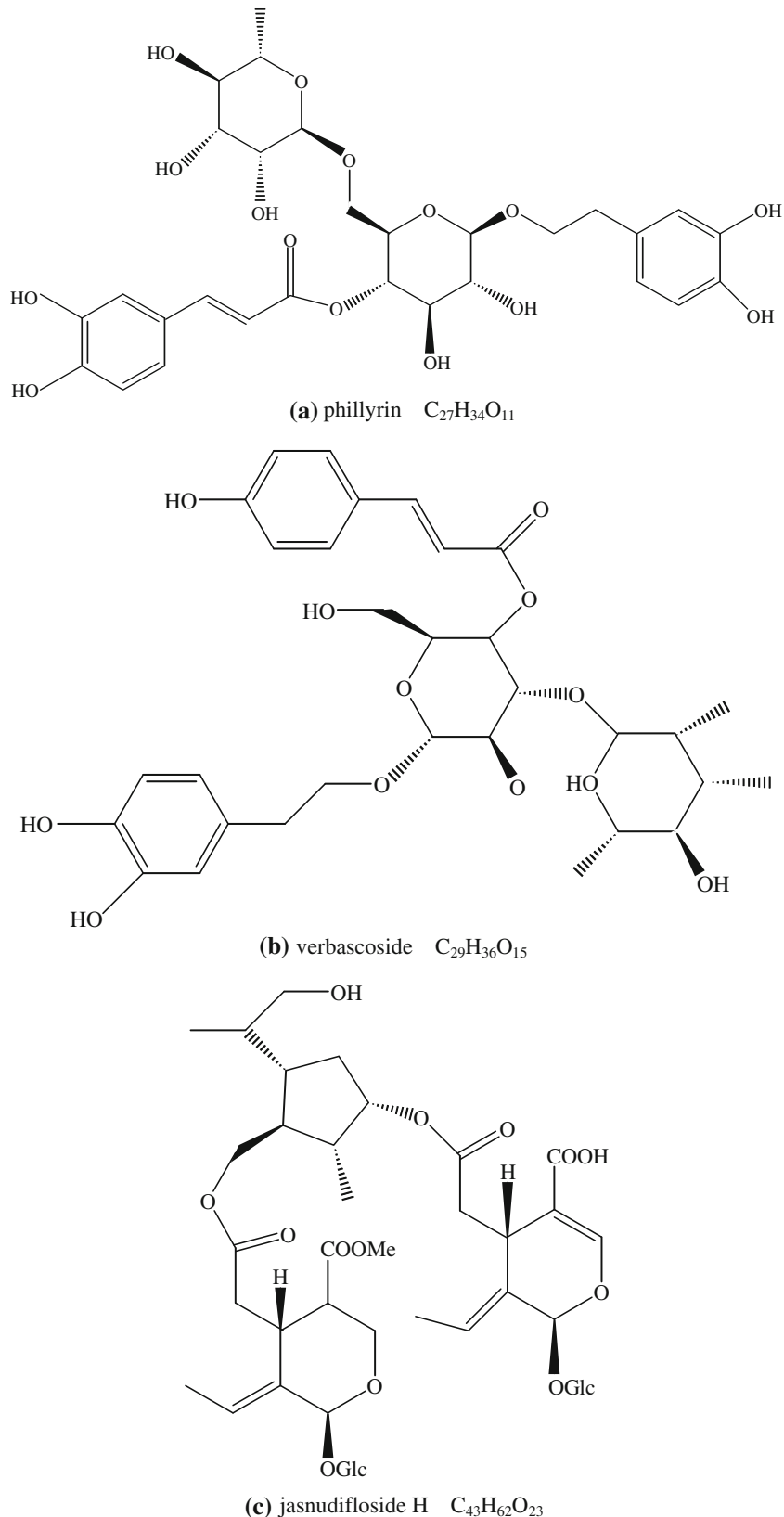
3.7 Explanation for inhibition

JNLLE is composed of numerous naturally occurring organic compounds. The inhibitive action of JNLLE toward the acid corrosion of steel can be attributed to the adsorption of its components of JNLLE onto the steel surface. The important constituents of extract are flavonoids of phillyrin ($C_{27}H_{34}O_{11}$), and verbascoside ($C_{29}H_{36}O_{15}$) [22], and secoiridoid glucoside of jasnudifloside H ($C_{43}H_{62}O_{23}$) [38], and the chemical structures are shown in Fig. 9. FTIR result also shows that JNLLE contains oxygen and nitrogen atoms in functional groups (O–H, N–H, C=C, C=O, C=N, C–N, C–O) and aromatic ring, which meets the general consideration of typical corrosion inhibitors. JNLLE might be protonated in the acid media as follows:



Thus, in aqueous acidic solutions, the JNLLE exists either as neutral molecules or in the form of cations (protonated JNLLE). In general, two modes of adsorption could be considered. The neutral JNLLE may adsorb on the metal surface via the chemisorption mechanism, involving the displacement of water molecules from the metal surface and the sharing electrons between the N and O atoms and Fe. The JNLLE molecules can also adsorb on the metal surface on the basis of donor–acceptor interactions between π -electrons of aromatic ring and vacant d-orbitals of Fe. On the other hand, it is well known that the steel surface charges positive charge in acid solution [39], so it is difficult for the protonated JNLLE to approach the positively charged steel surface (H_3O^+ /metal interface) due to the electrostatic repulsion. Since chloride ions have a smaller degree of hydration, being specifically adsorbed, they create an excess negative charge toward the solution and favor more adsorption of the cations [1], the protonated JNLLE may adsorb through electrostatic interactions between the positively charged molecules and the negatively charged metal surface. In other words, there may be a synergism

Fig. 9 Chemical structures of **a** phillyrin, **b** verbascoside, and **c** jasnudifloside H



between Cl^- and JNLLE, which improves the inhibitive capability of the inhibitor. When protonated JNLLE is adsorbed on metal surface, a coordinate bond may be

formed by partial transference of electrons from polar atoms (N and O atoms) to the metal surface. In addition, owing to lone-pair electrons of N and O atoms in JNLLE, JNLLE or

protonated JNLLE may combine with freshly generated Fe^{2+} ions on steel surface forming metal inhibitor complexes:



These complexes might get adsorbed onto steel surface by van der Waals force to form a protective film to keep CRS from corrosion. This assumption could be further confirmed by the FTIR results. SEM results prove that JNLLE could adsorb onto steel surface to form a denser and more tightly protective film. The film covers both anodic and cathodic reactive sites on the steel surface, and inhibits both reactions at the same time.

4 Conclusions

- (1) JNLLE is a very good inhibitor of corrosion of CRS in 1.0 M HCl. Inhibition efficiency value increases with the inhibitor concentration. The adsorption of JNLLE on CRS surface obeys the Langmuir adsorption isotherm.
- (2) JNLLE acts as a mixed-type inhibitor in 1.0 M HCl, and the inhibition is caused by geometric blocking effect. EIS spectra exhibit one capacitive loop which indicates that the corrosion reaction is controlled by charge transfer process. The addition of JNLLE in 1.0 M HCl solution enhances R_t values while reduces C_{dl} values.
- (3) FTIR and SEM results clearly show that JNLLE inhibits corrosion of steel by being adsorbed on the metal surface.

Acknowledgments This study was carried out in the scope of research project funded by Key Laboratory for Forest Resources Conservation and Use in the Southwest Mountains of China (Southwest Forestry University) Ministry of Education, Key Construction Course of Chemical Engineering for Forest Products of Southwest Forestry University (XKX200907). The electrochemical measurements were carried out using PARSTAT 2273 advanced electrochemical system (Princeton Applied Research) provided by Advanced Science Instrument Sharing Center of Southwest Forestry University.

References

1. Bentiss F, Traisnel M, Lagrenée M (2000) Corros Sci 42:127
2. Trabanelli G (1991) Corrosion 47:410
3. Singh DDN, Singh TB, Gaur B (1995) Corros Sci 37:1005
4. Zhang TS (2002) Corrosion inhibitors. Chemical Industrial Engineering Press, Beijing (in Chinese)
5. Ekpe UJ, Ebenso EE, Ibok UJ (1994) J West African Assoc 37:13
6. Loto CA (1998) Niger Corros J 19:20
7. Al-Sehaibani H (2000) Mater Wissen Werkst Technol 31:1060
8. Chetouani A, Hammouti B (2001) Bull Electrochem 19:23
9. Orubite KO, Oforka NC (2004) Mater Lett 58:1768
10. Gunasekaran G, Chauhan LR (2004) Electrochim Acta 49:4387
11. Chuanhan LR, Gunasekaran G (2007) Corros Sci 49:1143
12. Abdel-Gaber AM, Abd-El Nabey BA, Sidahmed IM, El-Zayady AM, Saadawy M (2006) Corrosion 62:293
13. Bouyanzer A, Hammouti B, Majidi L (2006) Mater Lett 60:2840
14. El-Etre AY (2007) J Colloid Interface Sci 314:578
15. Okafor PC, Ikpi ME, Uwah IE, Ebenso EE, Ekpe UJ, Umores SA (2008) Corros Sci 50:2310
16. Oguzie EE (2008) Corros Sci 50:2993
17. Oguzie EE (2006) Mater Chem Phys 99:441
18. Abdel-Gaber AM, Abd-El-Nabey BA, Saadawy M (2009) Corros Sci 51:1038
19. Eddy NO, Odoemelam SA, Odiongenyi AO (2009) J Appl Electrochem 39:849
20. Raja PB, Sethuraman MG (2009) Mater Corros 60:22
21. Zheng MY, Wei YS (2003) Nat Prod Res Dev 15:494
22. Yang WB, Lu CY, Chen GX, Li GZ, Zhang M (2008) Food Sci 29:474 (in Chinese)
23. Zhang ZX (2000) J Wenshan Teach Coll 19:97 (in Chinese)
24. Li XH, Mu GN (2005) Appl Surf Sci 252:1254
25. Li XH, Deng SD, Fu H, Li TH (2009) Electrochim Acta 54:4089
26. Sekine I, Hirakawa Y (1986) Corrosion 42:272
27. Li XH, Deng SD, Fu H, Mu GN (2009) J Appl Electrochem 39:1125
28. Cao CN (2004) Corrosion electrochemistry mechanism. Chemical Engineering Press, Beijing, p 235 (in Chinese)
29. Larabi L, Harek Y, Traisnel M, Mansri A (2004) J Appl Electrochem 34:833
30. Lebrini M, Lagrenée M, Vezin H, Traisnel M, Bentiss F (2007) Corros Sci 49:2254
31. Priya ARS, Muralidharam VS, Subramania A (2008) Corrosion 64:541
32. Bommersbach P, Alemany-Dumont C, Millet JP, Normand B (2006) Electrochim Acta 51:4011
33. Qu Q, Jiang SA, Bai W, Li L (2007) Electrochim Acta 52:6811
34. Lagrenée M, Mernari B, Bouanis M, Traisnel M, Bentiss F (2002) Corros Sci 44:573
35. Lalitha A, Ramesh S, Rajeswari S (2005) Electrochim Acta 51:47
36. Manov S, Lamazouère AM, Ariès L (2000) Corros Sci 42:1235
37. Liao DW, Lin ZY, KhR Tsai (1996) J Xiamen Univ 35:734 (in Chinese)
38. Takenaka T, Tahanashi T, Taguchi H, Nagakura N (2002) Chem Pharm Bull 50:384
39. Tang LB, Li XM, Li L, Mu GN, Liu GH (2006) Surf Coat Technol 201:384